Chemistry & Biology, Vol. 11, 1719–1728, December, 2004, ©2004 Elsevier Ltd. All rights reserved. DOI 10.1016/j.chembiol.2004.10.009

Hydroxylated Polychlorinated Biphenyls Selectively Bind Transthyretin in Blood and Inhibit Amyloidogenesis: Rationalizing Rodent PCB Toxicity

Hans E. Purkey,[1] Satheesh K. Palaninathan,[2] Kathleen C. Kent,[1] Craig Smith,[2] Stephen H. Safe,[2] James C. Sacchettini,[2] and Jeffery W. Kelly[1,*]
[1]Department of Chemistry and
The Skaggs Institute for Chemical Biology
The Scripps Research Institute
La Jolla, California 92037
[2]Department of Biochemistry and Biophysics
Texas A&M University
College Station, Texas 77843

Summary

Polychlorinated biphenyls (PCBs) and their hydroxylated metabolites (OH-PCBs) are known to bind to transthyretin (TTR) in vitro, possibly explaining their bioaccumulation, rodent toxicity, and presumed human toxicity. Herein, we show that several OH-PCBs bind selectively to TTR in blood plasma; however, only one of the PCBs tested binds TTR in plasma. Some of the OH-PCBs displace thyroid hormone (T4) from TTR, rationalizing the toxicity observed in rodents, where TTR is the major T4 transporter. Thyroid binding globulin and albumin are the major T4 carriers in humans, making it unlikely that enough T4 could be displaced from TTR to be toxic. OH-PCBs are excellent TTR amyloidogenesis inhibitors in vitro because they bind to the TTR tetramer, imparting kinetic stability under amyloidogenic denaturing conditions. Four OH-PCB/TTR cocrystal structures provide further insight into inhibitor binding interactions.

Introduction

Polychlorinated biphenyls (PCBs) are known persistent environmental pollutants [1] that are reported to be toxic to rodents and possibly humans [2–4]. The longevity of these compounds in the environment is due to their slow degradation and high lipophilicity, which allows them to bioaccumulate and concentrate as they move up the food chain [2]. Hydroxylated PCBs (OH-PCBs) are metabolites formed by oxidation of PCBs by the P450 monooxygenases [5]. Definitive data on the toxicity of individual PCB compounds in humans is difficult to find due to the fact that the commercially available PCBs are generally mixtures that contain many different isomers as well as trace amounts of known toxins, e.g., chlorinated dibenzofurans [2]. However, the toxicity of several purified PCBs has been demonstrated in laboratory animals. Bone loss [6], immunologic toxicity [4], neurotoxicity [7, 8], and lowered thyroid hormone levels, in addition to the estrogenicity of the OH-PCBs [9, 10] are associated with the administration of these compounds.

Numerous studies demonstrate that PCBs and OH-PCBs bind to transthyretin (TTR) in vitro [11–17]. Transthyretin is a 127 residue β sheet-rich tetrameric protein present in human blood plasma (3.6 μM) and cerebrospinal fluid (CSF) (0.36 μM). TTR has two C_2-interconvertible thyroxine (T4) binding sites and four orthogonal holo-retinol binding protein binding sites, of which a maximum of two can be occupied due to overlapping footprints. It has been hypothesized that PCB and OH-PCB displacement of T4 from TTR causes lowered T4 levels in exposed rats and mice, as TTR is the primary T4 transporter in rodents. In human plasma, only 10%–15% of T4 is TTR bound because thyroxine binding globulin (TBG) and albumin are the main carriers [18–20]; in fact, less than 1% of human plasma TTR (≈3.6 μM) has T4 bound to it. It has been suggested that TTR is the protein target in human blood that contributes to the persistence of the OH-PCBs in exposed individuals [5]. While numerous reports implicate TTR as a PCB binding protein in vivo [21–25], there is no definitive evidence that PCBs bind to transthyretin in plasma. We have developed an antibody capture method that can be used to place a lower limit on the binding stoichiometry of small molecules to TTR in biological fluids [26]. The TTR binding stoichiometry of PCBs and OH-PCBs to human plasma TTR was evaluated herein.

Post-secretion amyloidogenesis of plasma TTR requiring rate-limiting tetramer dissociation, monomer misfolding, and misassembly putatively causes senile systemic amyloidosis, familial amyloid cardiomyopathy, and the familial amyloid polyneuropathies, a subset of which exhibit CNS symptoms [27–36]. Several structurally diverse groups of compounds have been identified by screening and structure-based design that inhibit TTR amyloid formation in vitro [34, 37–48]. Herein, we demonstrate that several OH-PCBs bind selectively to TTR in human plasma and inhibit amyloid fibril formation through tetramer stabilization, leading to partial or complete kinetic stabilization of the native state [34]. Four representative TTR•$(OH\text{-}PCB)_2$ complexes were characterized by X-ray crystallography to better understand the molecular basis for binding and to provide the basis for the design of optimized TTR amyloidogenesis inhibitors.

Results

Binding Selectivity of PCBs and OH-PCBs for Transthyretin in Human Blood Plasma

The binding selectivity of eight PCBs (compounds **1–8**, Figure 1A), reported to displace thyroid hormone from TTR with an IC_{50} of less than 50 nM [17], and 14 OH-PCBs (compounds **9–22**, Figure 1B), known PCB metabolites that are reported to bind to TTR [12, 14–16, 49] or lower thyroxine levels in mice or rats [22, 50], was evaluated using an established method [26]. Lower limits on PCB binding stoichiometry to TTR in plasma were established using polyclonal TTR antibodies covalently attached to a Sepharose resin that was mixed with human blood plasma pretreated with PCB or OH-

*Correspondence: jkelly@scripps.edu

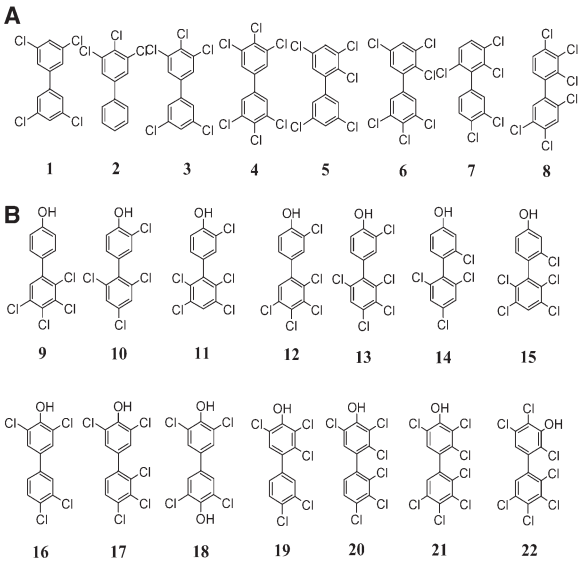

Figure 1. Compounds Evaluated in This Study

Structures of the PCBs (A) and OH-PCBs (B) screened for binding to TTR in blood plasma.

PCB (10.8 μM). After washing with 0.05% saponin in buffer and just pH 8 buffer, the PCB or OH-PCB binding stoichiometry to TTR (≈5 μM) was evaluated by reverse phase HPLC [26].

Up to two PCBs can bind to the two identical thyroid hormone binding sites in the TTR tetramer. Except for PCBs **1** and **3**, the remaining nonhydroxylated PCBs displayed relatively low binding selectivity for plasma TTR (<0.2; Table 1). In contrast, the OH-PCBs showed good to excellent binding selectivity for plasma TTR (0.7–1.9 stoichiometry; Table 1). Several of the hydroxylated PCBs (e.g., **16**, **17**, **19**, and **22**) exhibit a binding stoichiometry exceeding 1.5. The binding selectivity of OH-PCBs in blood is similar to that observed in plasma (Table 1); hence, erythrocyte membranes do not significantly sequester the OH-PCBs studied.

Table 1. Binding Stoichiometry of PCBs and OH-PCBs to Transthyretin in Human Plasma and Blood, Uncorrected for Losses that May Occur during Five Wash Steps

Compound	Equivalents Bound (Plasma)	Equivalents Bound (Blood)
1	0.62 ± 0.12	ND
2	0.18 ± 0.03	ND
3	1.50 ± 0.42	ND
4	0.05 ± 0.04	ND
5	0.06 ± 0.04	ND
6	0.19 ± 0.11	ND
7	no binding	ND
8	no binding	ND
9	0.83 ± 0.19	0.57
10	0.96 ± 0.09	0.93
11	1.12 ± 0.22	1.20
12	1.23 ± 0.24	1.47
13	0.84 ± 0.24	0.86
14	0.81 ± 0.29	0.73
15	0.70 ± 0.17	0.56
16	1.86 ± 0.14	ND
17	1.63 ± 0.05	ND
18	1.36 ± 0.21	ND
19	1.48 ± 0.16	1.55
20	1.02 ± 0.09	0.86
21	1.40 ± 0.22	1.33
22	1.67 ± 0.40	1.69

ND, not determined.

The antibody capture of the TTR•PCB complex underestimates the PCB binding stoichiometry in plasma owing to PCB dissociation from TTR during the five wash steps, three with 0.05% saponin in pH 8 buffer and two with pH 8 buffer. Selected PCBs and OH-PCBs (10.8 μM) were incubated with recombinant TTR (3.6 μM) to evaluate the stoichiometry of small molecule bound to immobilized TTR after each wash step. Stoichiometry decreased by 10%–17% for PCB **2** and OH-PCB **18** after five washes (Figure 2A), whereas that of PCB **4** decreased by 45%. Quantification of wash-associated losses allows one to estimate the true binding stoichiometry of PCBs and OH-PCBs in plasma; however, uncorrected data are reported in Table 1, representing the lower limit of the binding stoichiometry in plasma or blood. Furthermore, a good correlation between the final stoichiometry of OH-PCB bound to recombinant TTR and the amount bound to TTR in plasma indicates that the compound is a highly selective TTR binder in plasma (after five wash steps), e.g., OH-PCB **18** (Figure 2B). In contrast, PCBs **2** and **4** exhibit a higher binding stoichiometry to TTR in buffer than in plasma, strongly suggesting that they bind to competitor protein(s) as well as TTR in plasma (Figure 2B).

TTR Amyloid Fibril Inhibition by Hydroxylated PCBs

The ability of OH-PCBs and PCB **3** (3.6 μM) to inhibit TTR amyloidogenesis in vitro was evaluated because these compounds exhibit good binding selectivity to TTR in blood. TTR secreted into blood from the liver appears to be the source of TTR amyloid in all diseases except the rare CNS disorders. While it is not yet clear where or how amyloid is formed in humans, acidic conditions are effective in converting nearly all amyloidogenic peptides and proteins into amyloid and/or related aggregates. Hence, acid-mediated (pH 4.4) fibril formation monitored by turbidity [38, 51] was employed to monitor the effectiveness of the PCBs as inhibitors. Hydroxylated PCBs and PCB **3** were highly efficacious as TTR fibril inhibitors (Figure 3). At an inhibitor concentration equal to the WT TTR concentration (3.6 μM), only 12%–50% of the normal amount of fibril formation was observed after a 72 hr incubation period. The activity at the lower end of this range is equivalent to that displayed by the best fibril inhibitors discovered to date [40, 42–44, 46–48], such as flufenamic acid [51], which was included as a positive control.

Binding of OH-PCB 18 to TTR

Previous mass spectrometry experiments suggest that OH-PCB **18** exhibits positively cooperative binding to TTR's two C_2-related thyroid hormone binding sites [52]. When substoichiometric (<1:1) amounts of **18** are added to TTR, the predominant species observed in the mass spectrometer are apo-TTR and the TTR•$\mathbf{18}_2$ complex, consistent with positively cooperative binding

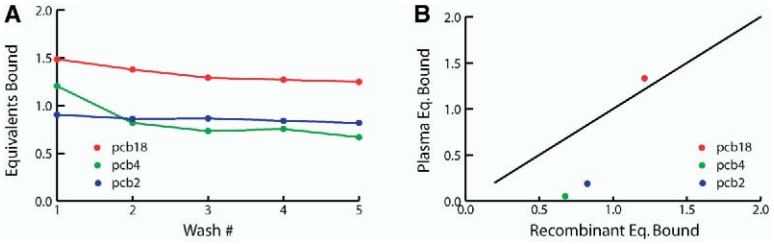

Figure 2. Determination of the Loss of Selected PCBs and OH-PCBs during the Five Wash Steps of the Immunocapture Method and Their Relative Binding Selectivities to TTR in Plasma and in Buffer

(A) Loss of PCBs **2**, **4**, and OH-PCB **18** during each wash step of the immunocapture method. The binding stoichiometry of the compounds after each step is shown.

(B) Correlation of the measured binding stoichiometry in plasma with the measured binding stoichiometry to recombinant TTR for selected PCBs and OH-PCB **18** using the immunoprecipitation method. The diagonal line represents a 1:1 correlation between the in vitro and plasma binding stoichiometries.

[52]. The TTR binding characteristics of **18** are in contrast to those exhibited by numerous other TTR amyloid fibril inhibitors that bind with negative cooperativity. Isothermal titration calorimetry studies carried out under physiological conditions reveal that the binding of OH-PCB **18** to WT TTR fits best to a model where the dissociation constants are identical (K_ds = 3.2 ± 1.8 nM). This result is not in contrast with positively cooperative binding, as one cannot achieve a low enough TTR concentration to probe positive cooperativity because of insufficient heat release. Attempts to fit the collected data to models of positively or negatively cooperative binding yielded poor fits.

Cocrystal Structures of OH-PCBs 12, 16, 17, **and** 18

Crystals of WT TTR bound by two equivalents of OH-PCBs **12**, **16**, **17**, and **18** were obtained by soaking TTR crystals with a 10-fold excess of inhibitor for 4 weeks. X-ray structures were then solved for each of the complexes (Table 2; Figure 4). The TTR dimer within the crystallographic asymmetric unit forms half of the two ligand binding pockets. Because both binding sites are bisected by the same 2-fold axis of symmetry, two symmetry equivalent binding modes of the inhibitors are typically observed (green and gray stick representations in Figure 4) [43, 44, 47, 48, 51]. Each TTR binding site can be subdivided into inner and outer cavities. These cavities comprise three so-called halogen binding pockets (HBPs) because they are occupied by the iodines on the two aromatic rings of thyroxine. HBP 3 and 3′ are located deep within the inner binding cavity, HBP 2 and 2′ define the boundary between the inner and outer binding cavity, whereas HBP 1 and 1′ are located near the periphery of outer binding cavity (Figure 4). The cocrystal structures reveal that the C-C bond connecting the two aromatic rings of the OH-PCB is nearly centered on the 2-fold symmetry axis, giving the appearance of a single binding conformation. The dihedral angle between two phenyl rings is 59° for **12**, 37° for both **16** and **17**, and 44° for **18**. All of the OH-PCBs occupy similar positions in the inner and outer binding pockets. The van der Waals complimentarity of the biaryl ring system facilitates several intersubunit interactions involving residues 108, 119, and 121 in the subunits comprising each binding site. Several of the substituents on the phenyl rings are off-axis and can be modeled in multiple positions within the observed electron density.

OH-PCB 18 **Bound to TTR**

The 1.8 Å X-ray crystal structure of the TTR•$\mathbf{18}_2$ complex demonstrates that the inhibitor has excellent steric complementarity with the TTR binding site (Figure 4A). Symmetrical inhibitor **18** makes hydrophobic contacts with the side chains of Leu17 and Ala108. Molecular mechanics (Insight II, Accelrys) indicates that the unbound preferred conformation of **18** is very close to its bound structure. The refined structure defines direct and water-mediated electrostatic interactions that contribute to high-affinity binding of **18**. One of the 3-Cl, 4-OH, 5-Cl identically substituted aromatic rings occupies the inner binding pocket, its chlorine substituents projecting into HBP 3 and 3′. The side chains of Ser117 and Thr119 adopt alternative conformations by rotation

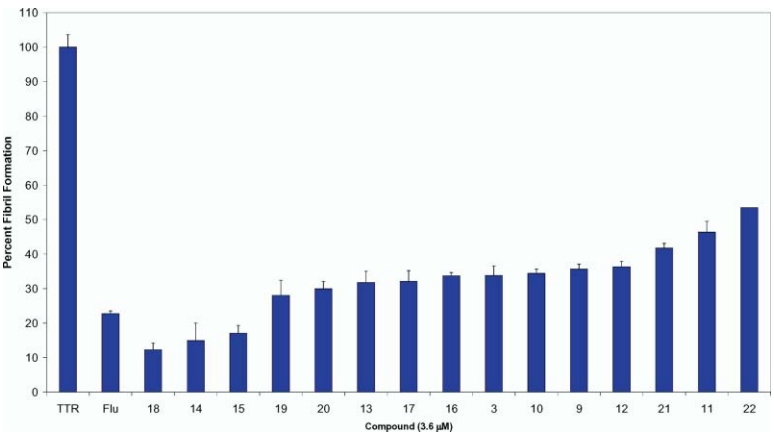

Figure 3. OH-PCB Inhibition of TTR Fibril Formation

OH-PCB inhibition (3.6 μM) of acid-mediated TTR (3.6 μM) fibril formation (pH 4.4) in vitro. TTR amyloidogenesis in the absence of inhibitor is assigned to be 100%. Flufenamic acid (Flu 3.6 μM) is included as a positive control.

Table 2. Refinement Statistics for OH-PCB•TTR Crystal Structures

	12	16	17	18
Unit cell parameters (Å)	42.62, 85.17, 64.61	43.68, 85.46, 64.24	43.68, 85.46, 64.24	43.68, 85.46, 64.24
Space group	$P2_12_12$	$P2_12_12$	$P2_12_12$	$P2_12_12$
Resolution (Å)	27.0–2.1	9.0–1.85	9.0–1.85	10.0–1.8
No. of unique reflections measured	14,176	18,746	19,133	21,209
Completeness (%) (overall/outer shell)	98.6/98.2	90.5/87.5	89.2/92.0	92.6/92.0
R_{sym} (overall/outer shell)	0.03/0.23	0.03/0.25	0.04/0.18	0.04/0.17
Refinement Statistics				
Resolution (Å)	27.0–2.1	9.0–1.85	9.0–1.85	10.0–1.8
R factor/R_{free} (%)	23.5/26.2	21.2/24.5	19.5/23.0	18.7/22.5

about their Cα-Cβ bonds as discerned by the unbiased electron density maps (Figure 4A). The side chain of Ser117 adopts all three low energy rotamer conformations as discerned by the distribution of electron density. Interestingly, two water molecules are located in between the adjacent Ser117 residues at the 2-fold axis with 50% occupancy, facilitating a network of hydrogen bonds connecting the Ser117 residues, the nearby water molecules, and the phenol functionality of **18** (Figure 4A). The two conformations of Thr119 confer electrostatic interactions that further stabilize the binding of **18**. In one conformation, the γ-O atom of Thr119 forms electrostatic interactions with the chlorine (3.4 Å) and a hydrogen bond with the side chain of Ser117 (2.6 Å), while in the second conformation it forms a hydrogen bond with a water molecule that also hydrogen bonds with three groups from TTR.

The other identically substituted ring occupies the outer TTR binding pocket with its halogens projecting into HBPs **1** and **1′**. It is not clear what role, if any, the hydroxyl substituent of **18** plays in binding, as the hydroxyl group does not form any H bonds with the protein or ordered solvent in the outer binding pocket. However, the Cl substituents appended to the ring in the outer binding pocket interact with an ordered water molecule that H bonds to the ε-ammonium group of Lys15.

OH-PCB 16 Bound to TTR

The 3-Cl, 4-OH, 5-Cl trisubstituted phenolic ring of **16** is oriented into the inner binding site of TTR, making the same electrostatic and hydrophobic interactions with TTR that this ring does in the TTR•18_2 structure described above (Figures 4A and 4B). The electron density of **16**, like that of OH-PCB **18**, is symmetric, and thus it is not possible to position the *para*-OH and *para*-

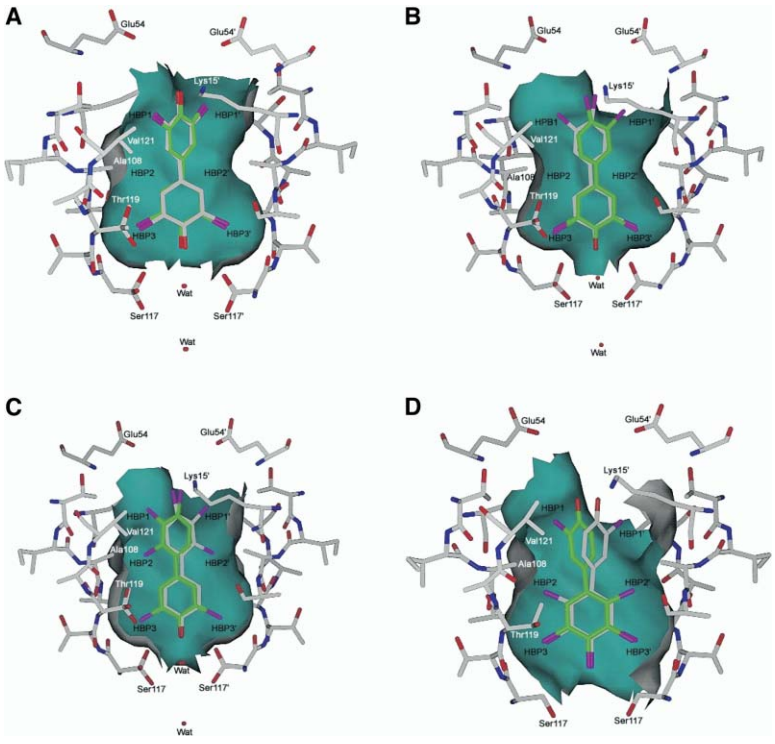

Figure 4. Cocrystal Structures of Selected OH-PCBs Bound to TTR

Depiction of compounds **18** (A), **16** (B), **17** (C), and **12** (D) bound to one of the two binding pockets of TTR shown as a surface. The center of the TTR tetramer (inner binding pocket) is at the bottom of each figure, and the solvent entrance to the pocket (outer binding pocket) is at the top. The two symmetry equivalent conformations of the small molecule are shown in gray and green. The halogen binding pockets are labeled as HBPs. Leu17 (A) is not shown for clarity.

Cl unambiguously based upon the electron density map. The unbiased electron density map is consistent with three rotomer conformations of Ser117, two conformations of Thr119, and contains two water molecules in between the Ser117 residues, analogous to the TTR•**18**$_2$ structure, apparently for the same function described above. The 3,4-dichlorinated aromatic ring occupies the outer binding pocket, with the halogen directed into HBP-1 or 1′, depending upon which symmetry equivalent binding mode is being considered (Figure 4B).

OH-PCB 17 Bound to TTR

Inhibitor **17** binds with its 3-Cl, 4-OH, 5-Cl substituted aryl ring oriented into the inner binding pocket, utilizing the same interactions that this ring uses in the TTR•**16**$_2$ and TTR•**18**$_2$ structures described above (Figure 4C). The multiple conformations of Ser117, Thr119, and the two conserved water molecules characterizing the structures described above are also features of the TTR•**17**$_2$ complex, presumably for the same reasons. The 2,3,4-trichlorinated ring occupies the outer binding pocket, utilizing interactions with HBP-1 and HBP-2 or the symmetry equivalents HBP1′ and HBP-2′.

OH-PCB 12 Bound to TTR

Biaryl **12** places its 3-Cl, 4-OH substituted aryl ring in the outer binding pocket, with the chlorine substituent interacting with HBP-1 or 1′ (Figure 4D), in contrast to the structures of TTR•**16**$_2$ and TTR•**17**$_2$, where the phenol-substituted ring is located in the inner binding pocket. The hydroxyl group (probably in the ionized form) is within hydrogen bonding distance of the Lys15 side chains, justifying its orientation in the outer binding site. The tetrachlorinated ring is placed in the inner binding pocket wherein the halogens are oriented in HBPs 3, 3′ and 2′, or 3′, 3 and 2. The Ser117 and Thr119 side chains adopt conformations that are identical to those found in the apo-TTR structure, unlike the situation in **16**, **17**, and **18**.

Discussion

Although it has been known for some time that PCBs and OH-PCBs bind to TTR in vitro [12, 14–17, 49], there has been very little direct evidence that these compounds can bind TTR selectively in plasma or CSF in vivo. Most in vivo studies have monitored this interaction indirectly through the levels of thyroid hormone [13, 23, 53–58], which is problematic because albumin binding can also displace T4. The only studies showing evidence of OH-PCB binding to TTR in plasma utilized a radiolabeled OH-PCB and reported that **16** migrated at the position of TTR on a native polyacrylamide gel of whole plasma [22, 24, 25].

Herein, we evaluated eight PCBs previously reported to displace T4 with an IC_{50} of less than 50 nM and show that only **1** and **3** bind to TTR with an appreciable stoichiometry in human plasma (Table 1). In contrast, all 14 OH-PCBs previously reported to bind to TTR exhibited excellent binding selectivity to TTR in plasma, with nine exhibiting binding stoichiometries exceeding 1 (Table 1). This is consistent with the observation that OH-PCBs are observed primarily in plasma and appear to be selectively retained there, as opposed to sequestration by lipids and other tissues where PCBs typically accumulate [5]. The OH-PCBs also bind selectively to TTR in whole blood, consistent with the idea that they do not partition into lipid membranes of erythrocytes (Table 1).

The amount of PCB (or OH-PCB) that washes off of the antibody•TTR•PCB complex during the five washing steps of the antibody capture method was evaluated using recombinant WT TTR (Figure 2) [26]. The extent of wash-associated PCB dissociation is molecule specific. Some compounds exhibit high binding stoichiometry after the washes, consistent with high initial binding selectivity and low wash-associated losses, implying a slow dissociation rate. Compounds exhibiting low binding stoichiometry fall into at least two categories: those with high initial binding stoichiometry exhibiting significant wash-associated losses or those displaying low initial binding stoichiometry without significant wash-associated losses, the latter scenario applicable to compounds that bind with high affinity to TTR but with even higher affinity to another plasma protein(s). PCBs **2** and **4** both exhibit low post-wash binding stoichiometry to recombinant TTR (Figure 2). Forty-five percent of PCB **4** was lost due to washes, whereas PCB **2** simply exhibits poor initial binding stoichiometry with minimal wash-associated losses (10%). The post-wash stoichiometry values reported in Table 1 reflect a lower limit of the amount of PCB that is initially bound in plasma because they are not corrected for wash-associated losses. Compounds like OH-PCB **18**, which are characterized by high post-wash binding stoichiometry, must exhibit high binding affinity selectivity and a slow dissociation rate, consistent with the slow off-rate observed [34]. These are the type of molecules that are the most useful native state stabilizers [34, 37].

In addition to their high binding selectivity to plasma TTR, the OH-PCBs and PCB **3** also display excellent inhibition of TTR fibril formation in vitro (Figure 3). The efficacy of inhibitors **14**, **15**, and **18** are among the highest observed to date at equimolar inhibitor and TTR concentration (3.6 μM). This is likely attributable to their high binding affinity and their slow dissociation rates and their non- or positively cooperative TTR binding properties, which are unusual [34, 37, 44, 51, 52, 59]. The calorimetric data do not allow one to distinguish between positively and noncooperative binding; however, we will assume the latter, which seems to better explain the data reported below. The nM K_ds exhibited by the best inhibitor, OH-PCB **18**, dictate that the native state of TTR will be stabilized by >3 kcal/mol. Selective ground state stabilization by **18** relative to the dissociative transition state raises the tetramer dissociation barrier substantially, such that the tetramer cannot dissociate on a biologically relevant timescale [34]. Since tetramer dissociation is required for amyloidogenicity, kinetic stabilization of the native state prevents aggregation. Kinetic stabilization of the native state mediated by binding of **18** was confirmed by the dramatically slowed tetramer dissociation rates in 6 M urea and sluggish amyloidogenicity at pH 4.4 [34]. We propose that the noncooperative binding of OH-PCB **18** (3.6 μM)

conveys kinetic stabilization on the tetramer, i.e., it raises the kinetic barrier of dissociation by selective stabilization of the ground state over the dissociative transition state [34]. In other words, kinetic stabilization of TTR by the binding of **18** prevents 2/3 of a 3.6 μM TTR sample from being amyloidogenic at pH 4.4 because TTR•**18** and TTR•$\mathbf{18}_2$ are incompetent to form amyloid; the remainder of TTR (≈1.18 μM) forms amyloid very inefficiently because of its low concentration [34, 60]. The dissociation rates of the best OH-PCB inhibitors may also be slower than expected because of TTR structural annealing around the OH-PCB, but this has not yet been evaluated as carefully as required. At a minimum, these compounds provide guidance for the synthesis of exceptional inhibitors or may themselves prove useful as inhibitors, depending on their toxicity profile.

The structures of OH-PCBs **12**, **16**, **17**, and **18** bound to TTR reveal that these biaryls generally bind along the crystallographic 2-fold symmetry axis. The dihedral angle between the two rings ranges from ~40°–60°, allowing the halogen binding pockets on two neighboring subunits to be engaged simultaneously, leading to stabilization of the tetrameric quaternary structural interface. For example, hydroxylated PCB **18** has optimal structural complimentarity with TTR, as its chlorines are able to bind to HBPs 1 and 1′ as well as 3 and 3′ simultaneously.

The orientation of the phenolic ring into the inner binding pocket appears to play an important role in that it enables a water-mediated hydrogen bonding network to form between it and neighboring TTR subunits, which presumably further stabilizes the native quaternary structure of TTR. An H-bonding network involving the three staggered conformations of Ser117, the phenolic group of the inhibitor, and the two conserved water molecules creates an electrostatic network that interconnects the two subunits that form the PCB binding site. In contrast, this network of electrostatic interactions is absent in the $\mathbf{12}_2$•TTR complex, in which the hydroxyl substituted phenyl ring is oriented in the outer binding pocket. Therefore, Ser117 and Thr119 in the inner binding pocket adopt apo side chain conformations in the $\mathbf{12}_2$•TTR structure. While there are differences in the TTR•OH-PCB cocrystal structures, these cannot be used alone to explain selectivity, as binding to proteins in addition to TTR must also be considered.

Surprisingly, the toxicity of OH-PCBs is not well established in the literature. In a variety of in vitro and animal studies, OH-PCBs appear to be either mildly estrogenic [10, 61–63] or antiestrogenic [7, 64–66]. Hydroxylated PCBs are also potent inhibitors of estrogen sulfotransferase activities and specifically inhibit SULT1E1 [67, 68]. It has been suggested that this inhibitory response may increase free 17b-estradiol levels, thereby indirectly enhancing estrogenic activity. Hydroxylated PCBs also inhibit sulfation and glucuronidation of benzo[a]pyrene [69] and exhibit weak thyroid hormone-like activity in a yeast two-hybrid assay [70]. Other toxicity mechanisms have been suggested [67, 71], and there are also reports of decreased thyroid hormone levels in animals exposed to these compounds. The suggestion that OH-PCB binding to TTR lowers T4 levels and that lowered T4 levels reflects small molecule TTR binding is difficult to directly support. Since >85% of T4 is carried by albumin and thyroid binding globulin, the displacement of T4 from these proteins seems more likely to be the cause of the lowered T4 levels in individuals exposed to PCBs. Thyroid binding globulin has the highest affinity for thyroxine and is a main carrier in humans [72], but it is not present in many lower mammals, including rats and mice [73], where many of the toxicological profiles of these compounds have been studied. Thus, in these species it is more likely that compounds binding to TTR will have an effect on the overall binding, transport, and levels of T4. Data showing binding of PCBs to TBG suggest little interaction, with the exception of one or two weakly binding compounds [15, 16]. Therefore, the effect of OH-PCBs on human thyroid levels should be minimal unless they bind to albumin. There are also reports that these compounds may interfere with thyroid hormone activation [74] or are associated with an increase in the rate of sulfation and therefore inactivation of T4 [75, 76]. OH-PCBs could also bind to other thyroid hormone targets including thyroid hormone receptors, which seems reasonable given the structural analogy with T4.

It is clear that little is established regarding OH-PCB toxicity, especially in humans. The toxicology in rodents is expected to be more severe, owing to the primary roles of albumin and TTR as the transporters. What is clear is that OH-PCBs exhibit excellent activity as inhibitors of transthyretin fibril formation, suggesting that this class of compounds has the potential to be useful for the inhibition of amyloid fibril formation, provided that the toxicity of these compounds can be understood [77].

Significance

Herein, we demonstrate that hydroxylated polychlorinated biphenyls (OH-PCBs) bind with high affinity and selectivity to transthyretin in plasma and in blood. Many of the OH-PCBs are excellent amyloid fibril formation inhibitors in vitro owing to their ability to bind to the native state of transthyretin, kinetically stabilizing the tetramer against dissociation required for amyloidogenesis. X-ray cocrystal structures reveal that OH-PCBs make hydrophobic and electrostatic bridging interactions between the subunits that stabilize the native tetrameric state of transthyretin. Moreover, the best OH-PCB inhibitor binds non- or positively cooperatively to the two thyroxine binding sites within transthyretin, which seems to be an important attribute of an exceptional inhibitor, unlike the majority of inhibitors that bind with negative cooperativity. These compounds may be useful in humans if the toxicity of this class of compounds can be better understood. The administration of transthyretin amyloidogenesis inhibitors like the ones described within to transgenic animals and ultimately to humans will allow us to validate or disprove the amyloid hypothesis, the idea that the process of amyloid fibril formation causes the neurodegeneration characteristic of these disorders.

Experimental Procedures

Transthyretin Antibody Purification and Conjugation to Sepharose

Antibodies were produced, purified, and coupled to Sepharose as reported [26]. The resin was stored as a 1:1 slurry in TSA (10 mM Tris [pH 8.0]/140 mM NaCl/0.025% NaN_3). Quenched Sepharose was prepared by coupling 200 mM Tris (pH 8.0) to the resin instead of the antibody.

Human Plasma Preparation

Whole blood was drawn from healthy volunteers at the Scripps General Clinical Research Center's Normal Blood-Drawing Program and transferred to 50 ml conical tubes. The tubes were centrifuged (1730 × g) in a Sorvall RT7 benchtop centrifuge equipped with a swinging bucket rotor for 10 min at 25°C. The plasma supernatant was removed and centrifuged again for 10 min to remove the remaining cells. Sodium azide was added to give a 0.05% solution. The plasma was stored at 4°C until used.

Immunoprecipitation of Transthyretin and Bound PCBs

A 2 ml tube was filled with 1.5 ml of human blood plasma and 7.5 μl of a 2.16 mM DMSO solution of the PCB under evaluation. This solution was incubated at 37°C for 24 hr. A 1:1 resin/TSA slurry (187 μl) of quenched Sepharose was added to the solution and gently rocked at 4°C for 1 hr. The solution was centrifuged (16,000 × g), and the supernatant was divided into three aliquots of 400 μl each. These were each added to 200 μl of a 1:1 resin/TSA slurry of the anti-transthyretin antibody-conjugated Sepharose and slowly rocked at 4°C for 20 min. The samples were centrifuged (16,000 × g), and the supernatant was removed. The resin was washed with 1 ml TSA/0.05% Saponin (Acros) (3× 10 min) at 4°C and additionally with 1 ml TSA (2× 10 min) at 4°C. The samples were centrifuged (16,000 × g), and the final wash was removed. One hundred fifty-five microliters of 100 mM triethylamine (pH 11.5) was added to the resin to elute the TTR and bound small molecules from the antibodies. Following gentle rocking at 4°C for 30 min, the samples were centrifuged (16,000 × g), and 145 μl of the supernatant, containing TTR and inhibitor, was removed.

HPLC Analysis and Quantification of Transthyretin and Bound PCBs

The supernatant remaining after centrifugation of the TTR antibody beads (145 μl) (described directly above) was loaded onto a Waters 71P autosampler. A 135 μl injection of each sample was separated on a Keystone 3 cm C18 reverse phase column utilizing a 40%–100% B gradient over 8 min (A, 94.8% H_2O/5% acetonitrile/0.2% TFA; B, 94.8% acetonitrile/5% H_2O/0.2% TFA) controlled by a Waters 600E multisolvent delivery system. Detection was accomplished at 280 nm with a Waters 486 tunable absorbance detector, and the peaks were integrated to give the area of both TTR and the small molecule. In order to determine the quantity of each species, known amounts of tetrameric TTR or PCB were injected onto the HPLC. The peaks were integrated to create calibration curves from linear regressions of the data using Kaleidagraph (Synergy Software). The calibration curves were used to determine the number of moles of each species present in the plasma samples. The ratio of small molecule to protein was calculated to yield the stoichiometry of small molecule bound to TTR in plasma.

Transthyretin Amyloid Fibril Formation Assay

Potential inhibitors were dissolved in DMSO at a concentration of 720 μM. Five microliters of a solution of the compound being evaluated was added to 0.5 ml of a 7.2 μM TTR solution in 10 mM phosphate (pH 7.6), 100 mM KCl, 1 mM EDTA buffer, allowing the compound to incubate with TTR for 30 min. Four hundred ninety-five microliters of 0.2 mM acetate buffer (pH 4.2), 100 mM KCl, 1 mM EDTA was added to yield final TTR and inhibitor concentrations of 3.6 μM each and a final pH of 4.4. The mixture was incubated at 37°C for 72 hr, after which the tubes were vortexed for 3 s, and the optical density was measured at 400 nm. The extent of fibril formation was determined by normalizing each optical density by that of TTR without inhibitor, defined to be 100% fibril formation. Control solutions of each compound in the absence of TTR were tested, and none absorbed appreciably at 400 nm.

Isothermal Titration Calorimetry of PCB 18 and TTR

A 25 μM solution of compound **18** (in 10 mM phosphate [pH 7.6], 100 mM KCl, 1 mM EDTA, 8% DMSO) was titrated into a 1.2 μM solution of TTR in an identical buffer using a Microcal MCS Isothermal Titration Calorimeter (Microcal, Northampton, MA). An initial injection of 2 μl was followed by 25 injections of 10 μl at 25°C. The thermogram was integrated, and a blank was subtracted to yield a binding isotherm that fit best to a model of two identical binding sites using the ITC data analysis package in ORIGIN 5.0 (Microcal).

Crystallization and X-Ray Data Collection

Crystals of recombinant WT TTR were obtained from protein solutions at 5 mg/ml (in 100 mM KCl, 100 mM phosphate [pH 7.4], 1 M ammonium sulfate) equilibrated against 2 M ammonium sulfate in hanging drop experiments. The TTR•ligand complexes were prepared from crystals soaked for 2 weeks with a 10-fold molar excess of the ligand to ensure saturation of both binding sites. 1:1 acetone:water solution was used as a soaking agent. A DIP2030b imaging plate system (MAC Science, Yokohama, Japan) coupled to an RU200 rotating anode X-ray generator was used for data collection. The crystals were placed in paratone oil as a cryo-protectant and cooled to 120 K for the diffraction experiments. Crystals of all TTR•ligand complexes are isomorphous with the apo crystal form containing unit cell dimensions a = 43 Å, b = 86 Å, and c = 65 Å, α, β, γ = 90°. They belong to the space group $P2_12_12$ and contain half of the homotetramer in the asymmetric unit. Data were reduced with DENZO and SCALEPACK [78].

Structure Determination and Refinement

The protein atomic coordinates for TTR from the Protein Data Bank (accession number 1BMZ) were used as a starting model for the refinement of native TTR and the TTR-ligand complexes by molecular dynamics and energy minimization using the program CNS [79]. Maps were calculated from diffraction data collected on TTR crystals either soaked with PCBs or cocrystalized simultaneously. For the complexes of TTR with the PCBs, the resulting maps revealed approximate positions of the ligand in both binding pockets of the TTR tetramer, with peak heights of above 5–9 rms. In order to improve the small molecule electron density and remove the model bias, the model was subjected to several cycles of the shake/warp protocol [80–82], which resulted in improvement in the map, especially around the inhibitor. Subsequent model fitting was done using these maps, and the ligand molecule was placed into the density. In all three cases, the minimum-energy conformation of the inhibitor calculated by the program InsightII (Accelrys) was in good agreement with the bound conformation reflected by the map. Because of the 2-fold crystallographic symmetry axis along the binding channel, a statistical disorder model must be applied, giving rise to two ligand binding modes in each of the two binding sites of tetrameric TTR. Water molecules were added based upon the unbiased electron density map. Because of the lack of interpretable electron densities in the final map, the nine N-terminal and three C-terminal residues were not included in the final model. See Table 2 for a summary of the crystallographic analysis.

Acknowledgments

We thank Joel Buxbaum for helpful discussions and the National Institutes of Health grants DK46335, ESO9106, ESO4917, the Lita Annenberg Hazen Foundation, the Skaggs Institute of Chemical Biology, and a San Diego ARCS Foundation Fellowship (H.E.P.) for financial support of this work. J.W.K. is a cofounder of Fold Rx Pharmaceuticals, a company that is developing small-molecule amyloidogenesis inhibitors.

Received: March 23, 2004
Revised: October 12, 2004
Accepted: October 13, 2004
Published: December 17, 2004

References

1. Safe, S. (1992). Toxicology, structure-function relationship, and human and environmental health impacts of polychlorinated bi-

phenyls: progress and problems. Environ. Health Perspect. *100*, 259–268.
2. Safe, S.H. (1994). Polychlorinated biphenyls (PCBs): environmental impact, biochemical and toxic responses, and implications for risk assessment. Crit. Rev. Toxicol. *24*, 87–149.
3. Safe, S. (1996). Human toxicology of chlorinated organic micropollutants. Issues Environ. Sci. Technol. *6*, 73–88.
4. Koss, G., and Wolfle, D. (1999). Dioxin and dioxin-like polychlorinated hydrocarbons and biphenyls. In Toxicology, H. Marquardt, S.G. Schäfer, R. McClellan, and F. Welsch, eds. (New York: Academic Press), pp. 699–728.
5. Bergman, A., Klasson-Wehler, E., and Kuroki, H. (1994). Selective retention of hydroxylated PCB metabolites in blood. Environ. Health Perspect. *102*, 464–469.
6. Schaar, J., Bernstein, A., Kuchenhoff, A., Seliger, G., and Hein, W. (1999). Effects of polychlorinated biphenyls on bone growth. Organohalogen Compd. *42*, 369–370.
7. Connor, K., Ramamoorthy, K., and Safe, S. (1996). The effects of hydroxylated polychlorinated biphenyls (PCBs) on the immature rat and mouse uterus. Organohalogen Compd. *29*, 312–315.
8. Kodavanti, P.R.S., and Tilson, H.A. (1997). Structure-activity relationships of potentially neurotoxic PCB congeners in the rat. Neurotoxicology *18*, 425–441.
9. Nesaretnam, K., and Darbre, P. (1997). 3,5,3′,5′-tetrachlorobiphenyl is a weak estrogen agonist in vitro and in vivo. J. Steroid Biochem. Mol. Biol. *62*, 409–418.
10. Carlson, D.B., and Williams, D.E. (2001). 4-Hydroxy-2′,4′,6′-trichlorobiphenyl and 4-hydroxy-2′,3′,4′,5′-tetrachlorobiphenyl are estrogenic in rainbow trout. Environ. Toxicol. Chem. *20*, 351–358.
11. McKinney, J.D., Chae, K., Oatley, S.J., and Blake, C.C.F. (1985). Molecular interactions of toxic clorinated dibenzo-p-dioxins and dibenzofurans with thyroxine binding prealbumin. J. Med. Chem. *28*, 375–381.
12. Richenbacher, U., McKinney, J.D., Oatley, S.J., and Blake, C.C.F. (1986). Structurally specific binding of halogenated biphenyls to thyroxine transport protein. J. Med. Chem. *29*, 641–648.
13. Van den Berg, K.J., Van Raaij, J.A.G.M., Bragt, P.C., and Notten, W.R.F. (1991). Interactions of halogenated industrial chemicals with transthyretin and effects on thyroid hormone levels in vivo. Arch. Toxicol. *65*, 15–19.
14. Lans, M.C., Klasson-Wehler, E., Willemsen, M., Meussen, E., Safe, S., and Brouwer, A. (1993). Structure-dependent, competitive interaction of hydroxy-polychlorobiphenyls, -dibenzo-p-dioxins and -dibenzofurans with human transthyretin. Chem. Biol. Interact. *88*, 7–21.
15. Lans, M.C., Spiertz, C., Brouwer, A., and Koeman, J.H. (1994). Different competition of thyroxine binding to transthyretin and thyroxine-binding globulin by hydroxy-PCBs, PCDDs, and PCDFs. Eur. J. Pharmacol. *270*, 129–136.
16. Cheek, A.O., Kow, K., Chen, J., and McLachlan, J.A. (1999). Potential mechanisms of thyroid disruption in humans: interaction of organochlorine compounds with thyroid receptor, transthyretin, and thyroid-binding globulin. Environ. Health Perspect. *107*, 273–278.
17. Chauhan, K.R., Kodavanti, P.R.S., and McKinney, J.D. (2000). Assessing the role of ortho-substitution on polychlorinated biphenyl binding to transthyretin, a thyroxine transport protein. Toxicol. Appl. Pharmacol. *162*, 10–21.
18. Nilsson, S.F., Rask, L., and Peterson, P.A. (1975). Studies of thyroid hormone-binding proteins. J. Biol. Chem. *250*, 8554–8563.
19. Petitpas, I., Petersen, C.E., Ha, C.-E., Bhattacharya, A.A., Zunszain, P.A., Ghuman, J., Bhagavan, N.V., and Curry, S. (2003). Structural basis of albumin-thyroxine interactions and familial dysalbuminemic hyperthyroxinemia. Proc. Natl. Acad. Sci. USA *100*, 6440–6445.
20. Petersen, C.E., Ha, C.-E., Harohalli, K., Park, D., and Bhagavan, N.V. (1997). Mutagenesis studies of thyroxine binding to human serum albumin define an important structural characteristic of subdomain 2A. Biochemistry *36*, 7012–7017.
21. Sandau, C.D., Ramsay, M., and Norstrom, R.J. (2000). Implication of hydroxylated metabolites of PCBs and other halogenated phenolic compounds as endocrine disruptors in polar bears. Proc. 3rd Bienn. Int. Conf. Monit. Meas. Environ., Chemistry Dept., Carleton University, Ottawa, Ontario, 47–52.
22. Darnerud, P.O., Morse, D., Klasson-Wehler, E., and Brouwer, A. (1996). Binding of a 3,3′,4,4′-tetrachlorobiphenyl (CB-77) metabolite to fetal transthyretin and effects on fetal thyroid hormone levels in mice. Toxicology *106*, 105–114.
23. Lans, M.C., Brouwer, I., de Winden, P., and Brouwer, A. (1993). Different effects of 2,3,7,8-tetrachlorodibenzo-p-dioxin and Aroclor 1254 on thyroxine metabolism and transport. Organohalogen Compd. *13*, 137–140.
24. Brouwer, A., Van den Berg, K.J., Blaner, W.S., and Goodman, D.S. (1986). Transthyretin (prealbumin) binding of PCBS, a model for the mechanism of interference with vitamin A and thyroid hormone metabolism. Chemosphere *15*, 1699–1706.
25. Brouwer, A., and Van den Berg, K.J. (1986). Binding of a metabolite of 3,4,3′,4′-tetrachlorobiphenyl to transthyretin reduces serum vitamin A transport by inhibiting the formation of the protein complex carrying both retinol and thyroxin. Toxicol. Appl. Pharmacol. *85*, 301–312.
26. Purkey, H.E., Dorrell, M.I., and Kelly, J.W. (2001). Evaluating the binding selectivity of transthyretin amyloid fibril inhibitors in blood plasma. Proc. Natl. Acad. Sci. USA *98*, 5566–5571.
27. Colon, W., and Kelly, J.W. (1992). Partial denaturation of transthyretin is sufficient for amyloid fibril formation in vitro. Biochemistry *31*, 8654–8660.
28. Lai, Z., Colon, W., and Kelly, J.W. (1996). The acid-mediated denaturation pathway of transthyretin yields a conformational intermediate which can self-assemble into amyloid. Biochemistry *35*, 6470–6482.
29. Lashuel, H.A., Lai, Z., and Kelly, J.W. (1998). Characterization of the transthyretin acid denaturation pathways by analytical ultracentrifugation: implications for wild-type, V30M, and L55P amyloid fibril formation. Biochemistry *37*, 17851–17864.
30. Liu, K., Cho, H.S., Lashuel, H.A., Kelly, J.W., and Wemmer, D.E. (2000). A glimpse of a possible amyloidogenic intermediate of transthyretin. Nat. Struct. Biol. *7*, 754–757.
31. Liu, K., Cho, H.S., Hoyt, D.W., Nguyen, T.N., Olds, P., Kelly, J.W., and Wemmer, D.E. (2000). Deuterium-proton exchange on the native wild-type transthyretin tetramer identifies the stable core of the individual subunits and indicates mobility at the subunit interface. J. Mol. Biol. *303*, 555–565.
32. Hammarström, P., Jiang, X., and Kelly, J.W. (2002). Sequence dependent denaturation energetics: a major determinant in amyloid disease diversity. Proc. Natl. Acad. Sci. USA *99*, 16427–16432.
33. Hammarstrom, P., Schneider, F., and Kelly, J.W. (2001). Trans-suppression of misfolding in an amyloid disease. Science *293*, 2459–2461.
34. Hammarstrom, P., Wiseman, R.L., Powers, E.T., and Kelly, J.W. (2003). Prevention of transthyretin amyloid disease by changingprotein misfolding energetics. Science *299*, 713–716.
35. Hammarstroem, P., Sekijima, Y., White, J.T., Wiseman, R.L., Lim, A., Costello, C.E., Altland, K., Garzuly, F., Budka, H., and Kelly, J.W. (2003). D18G transthyretin is monomeric, aggregation prone, and not detectable in plasma and cerebrospinal fluid: a prescription for central nervous system amyloidosis? Biochemistry *42*, 6656–6663.
36. Sekijima, Y., Hammarstroem, P., Matsumura, M., Shimizu, Y., Iwata, M., Tokuda, T., Ikeda, S.-i., and Kelly, J.W. (2003). Energetic characteristics of the new transthyretin variant A25T may explain its atypical central nervous system pathology. Lab. Invest. *83*, 409–417.
37. Cohen, F.E., and Kelly, J.W. (2003). Therapeutic approaches to protein-misfolding diseases. Nature *426*, 905–909.
38. Miroy, G.J., Lai, Z., Lashuel, H., Peterson, S.A., Strang, C., and Kelly, J.W. (1996). Inhibiting transthyretin amyloid fibril formation via protein stabilization. Proc. Natl. Acad. Sci. USA *93*, 15051–15056.
39. Baures, P.W., Peterson, S.A., and Kelly, J.W. (1998). Discovering transthyretin amyloid fibril inhibitors by limited screening. Bioorg. Med. Chem. *6*, 1389–1401.
40. Oza, V.B., Petrassi, H.M., Purkey, H.E., and Kelly, J.W. (1999).

Synthesis and evaluation of anthranilic acid-based transthyretin amyloid fibril inhibitors. Bioorg. Med. Chem. Lett. *9*, 1–6.
41. Baures, P.W., Oza, V.B., Peterson, S.A., and Kelly, J.W. (1999). Synthesis and evaluation of inhibitors of transthyretin amyloid formation based on the nonsteroidal antiinflammatory drug flufenamic acid. Bioorg. Med. Chem. *7*, 1339–1347.
42. Petrassi, H.M., Klabunde, T., Sacchettini, J., and Kelly, J.W. (2000). Structure-based design of N-phenyl phenoxazine transthyretin amyloid fibril inhibitors. J. Am. Chem. Soc. *122*, 2178–2192.
43. Klabunde, T., Petrassi, H.M., Oza, V.B., Raman, P., Kelly, J.W., and Sacchettini, J.C. (2000). Rational design of potent human transthyretin amyloid disease inhibitors. Nat. Struct. Biol. *7*, 312–321.
44. Oza, V.B., Smith, C., Raman, P., Koepf, E.K., Laushel, H.A., Petrassi, H.M., Chiang, K.P., Powers, E.T., Sacchettini, J.C., and Kelly, J.W. (2002). Synthesis, structure and activity of diclofenac analogs as transthyretin amyloid fibril inhibitors. J. Med. Chem. *45*, 321–332.
45. Sacchettini, J.C., and Kelly, J.W. (2002). Therapeutic strategies for human amyloid diseases. Nat. Rev. Drug Discov. *1*, 267–275.
46. Green, N.S., Palaninathan, S.K., Sacchettini, J.C., and Kelly, J.W. (2003). Synthesis and characterization of potent bivalent amyloidosis inhibitors that bind prior to transthyretin tetramerization. J. Am. Chem. Soc. *125*, 13404–13414.
47. Adamski-Werner, S.L., Palaninathan, S.K., Sacchettini, J.C., and Kelly, J.W. (2004). Diflunisal analogues stabilize the native state of transthyretin. Potent inhibition of amyloidogenesis. J. Med. Chem. *47*, 355–374.
48. Razavi, H., Palaninathan, S.K., Powers, E.T., Wiseman, R.L., Purkey, H.E., Mohamedmohaideen, N.N., Deechongkit, S., Chiang, K.P., Dendle, M.T.A., Sacchettini, J.C., et al. (2003). Benzoxazoles as transthyretin amyloid fibril inhibitors: Synthesis, evaluation, and mechanism of action. Angew. Chem. Int. Ed. Engl. *42*, 2758–2761.
49. Sandau, C.D., Meerts, I.A.T.M., Letcher, R.J., McAlees, A.J., Chittim, B., Brouwer, A., and Norstrom, R.J. (2000). Identification of 4-hydroxyheptachlorostyrene in polar bear plasma and its binding affinity to transthyretin: a metabolite of octachlorostyrene? Environ. Sci. Technol. *34*, 3871–3877.
50. Morse, D.C., Wehler, E.K., Wesseling, W., Koeman, J.H., and Brouwer, A. (1996). Alterations in rat brain thyroid hormone status following pre- and postnatal exposure to polychlorinated biphenyls (Aroclor 1254). Toxicol. Appl. Pharmacol. *136*, 269–279.
51. Peterson, S.A., Klabunde, T., Lashuel, H., Purkey, H., Sacchettini, J.C., and Kelly, J.W. (1998). Inhibiting transthyretin conformational changes that lead to amyloid fibril formation. Proc. Natl. Acad. Sci. USA *95*, 12956–12960.
52. McCammon, M.G., Scott, D.J., Keetch, C.A., Greene, L.H., Purkey, H.E., Petrassi, H.M., Kelly, J.W., and Robinson, C.V. (2002). Screening transthyretin amyloid fibril inhibitors—characterization of novel multiprotein, multiligand complexes by mass spectrometry. Structure *10*, 851–863.
53. Gould, J.C., Cooper, K.R., and Scanes, C.G. (1999). Effects of polychlorinated biphenyls on thyroid hormones and liver type I monodeiodinase in the chick embryo. Ecotoxicol. Environ. Saf. *43*, 195–203.
54. Crofton, K.M., Craft, E.S., Ross, D.J., and De Vito, M.J. (1998). Detecting the effects of environmental contaminants on thyroid hormones. A preliminary report on a short-term dosing model in the rat. Organohalogen Compd. *37*, 285–288.
55. Sinjari, T., and Darnerud, P.O. (1998). Hydroxylated polychlorinated biphenyls: placental transfer and effects on thyroxine in the fetal mouse. Xenobiotica *28*, 21–30.
56. Gould, J.C., Cooper, K.R., and Scanes, C.G. (1997). Effects of polychlorinated biphenyl mixtures and three specific congeners on growth and circulating growth-related hormones. Gen. Comp. Endocrinol. *106*, 221–230.
57. Sinjari, T., and Darnerud, P.O. (1995). Biochemical effects of hydroxylated PCB metabolites. Organohalogen Compd. *25*, 243–247.
58. Brouwer, A. (1989). Inhibition of thyroid hormone transport in plasma of rats by polychlorinated biphenyls. Arch. Toxicol. Suppl. *13*, 440–445.
59. Ferguson, R.N., Edelhoch, H., Saroff, H.A., and Robbins, J. (1975). Negative cooperativity in the binding of thyroxine to human serum prealbumin. Biochemistry *14*, 282–289.
60. White, J.T., and Kelly, J.W. (2001). Support for the multigenic hypothesis of amyloidosis: the binding stoichiometry of retinol-binding protein, vitamin A, and thyroid hormone influences transthyretin amyloidogenicity in vitro. Proc. Natl. Acad. Sci. USA *98*, 13019–13024.
61. Andersson, P.L., Blom, A., Johannisson, A., Pesonen, M., Tysklind, M., Berg, A.H., Olsson, P.E., and Norrgren, L. (1999). Assessment of PCBs and hydroxylated PCBs as potential xenoestrogens: in vitro studies based on MCF-7 cell proliferation and induction of vitellogenin in primary culture of rainbow trout hepatocytes. Arch. Environ. Contam. Toxicol. *37*, 145–150.
62. Schultz, T.W., Kraut, D.H., Sayler, G.S., and Layton, A.C. (1998). Estrogenicity of selected biphenyls evaluated using a recombinant yeast assay. Environ. Toxicol. Chem. *17*, 1727–1729.
63. Willett, K.L., and Safe, S.H. (1997). Hydroxylated polychlorinated biphenyls identified in human serum as inducers and inhibitors of EROD activity in the H4IIE cell bioassay. Organohalogen Compd. *34*, 172–177.
64. Connor, K., Ramamoorthy, K., Moore, M., Mustain, M., Chen, I., Safe, S., Zacharewski, T., Gillesby, B., Joyeux, A., and Balaguer, P. (1997). Hydroxylated polychlorinated biphenyls (PCBs) as estrogens and antiestrogens: structure-activity relationships. Toxicol. Appl. Pharmacol. *145*, 111–123.
65. Kramer, V.J., Helferich, W.G., Bergman, A., Klasson-Wehler, E., and Giesy, J.P. (1997). Hydroxylated polychlorinated biphenyl metabolites are anti-estrogenic in a stably transfected human breast adenocarcinoma (MCF7) cell line. Toxicol. Appl. Pharmacol. *144*, 363–376.
66. Moore, M., Mustain, M., Daniel, K., Chen, I., Safe, S., Zacharewski, T., Gillesby, B., Joyeux, A., and Balaguer, P. (1997). Antiestrogenic activity of hydroxylated polychlorinated biphenyl congeners identified in human serum. Toxicol. Appl. Pharmacol. *142*, 160–168.
67. Kester, M.H.A., Bulduk, S., Tibboel, D., Meinl, W., Glatt, H., Falany, C.N., Coughtrie, M.W.H., Bergman, A., Safe, S.H., Kuiper, G.G.J.M., et al. (2000). Potent inhibition of estrogen sulfotransferase by hydroxylated PCB metabolites: a novel pathway explaining the estrogenic activity of PCBs. Endocrinology *141*, 1897–1900.
68. Kester, M.H.A., Bulduk, S., Van Toor, H., Tibboel, D., Meinl, W., Glatt, H., Falany, C.N., Coughtrie, M.W.H., Schuur, A.G., Brouwer, A., et al. (2002). Potent inhibition of estrogen sulfotransferase by hydroxylated metabolites of polyhalogenated aromatic hydrocarbons reveals alternative mechanism for estrogenic activity of endocrine disrupters. J. Clin. Endocrinol. Metab. *87*, 1142–1150.
69. Van Den Hurk, P., Kubiczak, G.A., Lehmler, H.-J., and James, M.O. (2002). Hydroxylated polychlorinated biphenyls as inhibitors of the sulfation and glucuronidation of 3-hydroxy-benzo-[a]pyrene. Environ. Health Perspect. *110*, 343–348.
70. Shiraishi, F., Okumura, T., Nomachi, M., Serizawa, S., Nishikawa, J., Edmonds, J.S., Shiraishi, H., and Morita, M. (2003). Estrogenic and thyroid hormone activity of a series of hydroxy-polychlorinated biphenyls. Chemosphere *52*, 33–42.
71. Kuiper, G.G.J.M., Lemmen, J.G., Carlsson, B., Corton, J.C., Safe, S.H., Van Der Saag, P.T., Van Der Burg, B., and Gustafsson, J.-A. (1998). Interaction of estrogenic chemicals and phytoestrogens with estrogen receptor beta. Endocrinology *139*, 4252–4263.
72. Schreiber, G., and Richardson, S.J. (1997). The evolution of gene expression, structure and function of transthyretin. Comp. Biochem. Physiol. *116*, 137–160.
73. Larsson, M., Pettersson, T., and Carlstrom, A. (1985). Thyroid hormone binding in serum of 15 vertebrate species: isolation of thyroxine-binding globulin and prealbumin analogs. Gen. Comp. Endocrinol. *58*, 360–375.
74. Lans, M.C., and Klasson-Wehler, E. (1995). *In vitro* inhibition of thyroxine type 1-deiodinase by hydroxylated polychloro-biphe-

nyls, -dibenzo-*p*-dioxins and -dibenzofurans. PhD thesis, University of Waageningen, The Netherlands.

75. Schuur, A.G., Van Leeuwen-Bol, I., Jong, W.M.C., Bergman, A., Coughtrie, M.W.H., Brouwer, A., and Visser, T.J. (1998). In vitro inhibition of thyroid hormone sulfation by polychlorobiphenylols: isoenzyme specificity and inhibition kinetics. Toxicol. Sci. *45*, 188–194.
76. Schuur, A.G., Legger, F.F., van Meeteren, M.E., Moonen, M.J.H., van Leeuwen-Bol, I., Bergman, K., Visser, T.J., and Brouwer, A. (1998). In vitro inhibition of thyroid hormone sulfation by hydroxylated metabolites of halogenated aromatic hydrocarbons. Chem. Res. Toxicol. *11*, 1075–1081.
77. Teng, M.-H., Yin, J.-Y., Vidal, R., Ghiso, J., Kumar, A., Rabenou, R., Shah, A., Jacobson, D.R., Tagoe, C., Gallo, G., et al. (2001). Amyloid and nonfibrillar deposits in mice transgenic for wild-type human transthyretin: a possible model for senile systemic amyloidosis. Lab. Invest. *81*, 385–396.
78. Otwinowski, Z., and Minor, W. (1997). Processing of X-ray diffraction data collected in oscillation mode. Methods Enzymol. *276*, 307–326.
79. Brunger, A.T., Adams, P.D., Clore, G.M., DeLano, W.L., Gros, P., Grosse-Kunstleve, R.W., Jiang, J.-S., Kuszewski, J., Nilges, N., Pannu, N.S., et al. (1998). Crystallography & NMR system: a new software suite for macromolecular structure determination. Acta Crystallogr. D Biol. Crystallogr. *54*, 905–921.
80. Reddy, V., Swanson, S.M., Segelke, B., Kantardjieff, K.A., and Sacchettini, J.C. (2003). Acta Crystallogr. D Biol. Crystallogr. *59*, 2200–2210.
81. Bailey, S. (1994). The CCP4 suite: programs for protein crystallography. Acta Crystallogr. D Biol. Crystallogr. *50*, 760–763.
82. Murshudov, G.N., Vagin, A.A., and Dodson, E.J. (1997). Refinement of macromolecular structures by the maximum-likelihood. Methodol. Acta Crystallogr. D Biol. Crystallogr. *53*, 240–255.